

Generalized Wiener Estimation of Three-Dimensional Current Distribution from Biomagnetic Measurements

Sekihara, K.¹ and Scholz, B.²

¹Hitachi Central Research Laboratory, Tokyo, Japan; ²Siemens AG, Erlangen, Germany

Introduction

The inherent difficulty in the biomagnetic inverse problem is that a three-dimensional current distribution must be estimated from a biomagnetic field measured on a two-dimensional surface close to a human head or body. In such cases, the estimation is ill-posed. To reduce this ill-posedness, the current distribution to be estimated is often modeled by using the equivalent current dipole (ECD), which assumes a highly localized current source. However, when the source current distribution is not localized, or when no information regarding the spatial extent of the source distribution is obtained, we cannot rely on ECD modeling. The least-squares minimum-norm method [1] has been developed that does not use a particular source model and, therefore, can estimate non-localized sources. This method has been successfully applied in two-dimensional cases where the biocurrent distribution is assumed to be confined to a single or a few planes. Its three-dimensional application, however, poses a serious problem in that the signal current is estimated to be closer to the detector coils than its actual location [2]. This paper presents a method that can provide three-dimensional reconstruction where the conventional minimum-norm method fails. It utilizes the principle of the generalized Wiener estimation with the assumption that the activities of the biocurrent sources are uncorrelated.

Method

Let us define the magnetic field measured by the m th detector coil at time t_k as $b_m(t_k)$, and a vector $b(t_k) = (b_1(t_k), b_2(t_k), \dots, b_M(t_k))^T$ as a set of measured data at time t_k , $k = 1, 2, \dots, K$. Here, M is the total number of detector coils, K is the total number of time points, and the superscript T indicates the matrix transpose. Let us also define the signal primary current distribution at time t_k as a vector $f(t_k) = (f_1(t_k), f_2(t_k), \dots, f_{3N}(t_k))^T$. Here, N is the total number of pixels and the x , y , and z components of the primary current located at the i th pixel are assigned to $f_{3(i-1)+1}(t_k)$, $f_{3(i-1)+2}(t_k)$, and $f_{3(i-1)+3}(t_k)$, respectively. We define the lead field matrix L , which is a $M \times (3N)$ matrix. Its elements, $L_{m, 3(i-1)+1}$, $L_{m, 3(i-1)+2}$, and $L_{m, 3(i-1)+3}$, represent the sensitivity of the m th detector to the x , y , and z components of the primary current at the i th pixel. The column vector of the lead field matrix defined by $L_p = (L_{1p}, L_{2p}, \dots, L_{Mp})^T$ is introduced. The lead field matrix is expressed using its column vectors as, $L = (l_1, l_2, \dots, l_{3N})$. The relationship between $b(t_k)$ and $f(t_k)$ is given by $b(t_k) = L f(t_k) + n(t_k)$, where $n(t_k)$ is the noise vector. The m th element of this noise vector is the noise contained in the m th detector measurement at time t_k . The problem that this paper deals with is how to find the optimum estimate of the signal primary current source distribution $\hat{f}(t_k)$ at all time instants $k = 1, 2, \dots, K$, from a given spatio-temporal data set of measured data $b(t_k)$, $k = 1, 2, \dots, K$.

The method proposed in this paper utilizes the minimization of the following least-squares-error expressed in the source current space. That is, the cost function $\mathcal{F} = \sum_{k=1}^K \|f(t_k) - \hat{f}(t_k)\|^2$ is minimized to obtain the optimum estimate $\hat{f}(t_k)$. Here, $f(t_k)$ is the true current distribution at time t_k , and the measured data $b(t_k)$ is expressed as $b(t_k) = L f(t_k)$. The solution which minimizes the above cost function is known to be the generalized Wiener estimate or the minimum mean square error estimate [3]. This is expressed as $\hat{f}(t_k) = S L^T D^{-1} b(t_k)$. Here, defining the time average of A as $\langle A \rangle$, D is the covariance matrix of the measured data defined as $D = \langle b(t_k) b^T(t_k) \rangle$, and S is the covariance matrix of the signal current sources defined as $S = \langle f(t_k) f^T(t_k) \rangle$.

When applying the above equation to an actual problem, it is usually difficult to obtain an accurate estimate of the signal-source covariance matrix S . When all the non-diagonal elements of S can be

assumed to be zero, estimating the signal covariance matrix is performed in the following manner. Using the column vectors of the lead field matrix, let us express Wiener estimate as

$$\hat{f}_p(t_k) = S_{pp} l_p^T D^{-1} b(t_k), \quad (1)$$

where S_{pp} is the p th diagonal element of the signal covariance matrix. Defining the estimate of S_{pp} as \hat{S}_{pp} , we have

$$\hat{S}_{pp} = \langle \hat{f}_p(t_k) \hat{f}_p(t_k) \rangle = \langle (S_{pp} l_p^T D^{-1} b(t_k)) (S_{pp} l_p^T D^{-1} b(t_k))^T \rangle = S_{pp}^2 l_p^T D^{-1} l_p.$$

Assuming that $\hat{S}_{pp} = S_{pp}$, one can obtain the relationship $\hat{S}_{pp} = 1/(l_p^T D^{-1} l_p)$. Thus, the proposed Wiener estimation becomes

$$\hat{f}_p(t_k) = \frac{l_p^T D^{-1} b(t_k)}{l_p^T D^{-1} l_p}. \quad (2)$$

One problem with this estimation method is that it gives erroneous results when the orientations of current sources are completely fixed during the measurement. The extension of the methods to accommodate such cases can be performed in the following manner. Let us define the normal vector representing the orientation of the source current located at the p th pixel as e_p , and the $M \times 3$ matrix L_p as $L_p = [l_{3(p-1)+1}, l_{3(p-1)+2}, l_{3(p-1)+3}]$. This e_p can be obtained by solving the following eigenvalue problem at each pixel,

$$L_p^T D^{-1} L_p e_p = \lambda_{min} e_p, \quad (3)$$

where λ_{min} is the minimum eigenvalue. Once e_p is obtained, the amplitude of the current element at the p th pixel is obtained using

$$\hat{f}_p(t_k) = \frac{(L_p e_p)^T D^{-1} b(t_k)}{(L_p e_p)^T D^{-1} (L_p e_p)}. \quad (4)$$

Computer Simulation and Results

Computer simulations were performed to show the effectiveness of the proposed method. A magnetometer with thirty-seven channels that simulated the BTI 37-channel biomagnetic measurement system was assumed. The detector frame with its origin at the center of the coil alignment was used. The values of the coordinate (x, y, z) were expressed in centimeters. Since the homogeneous spherical conductor was assumed, only the two tangential components, ϕ and θ components, of the primary current vectors were considered.

Two time-varying magnetic-field sources were assumed to exist: the first source at $(-4, 1, -4)$ and the second source at $(3, 1, -6)$. This source configuration is schematically shown in Fig. 1. The ϕ and θ components of those sources randomly fluctuated, and the activities of the two sources were assumed to be uncorrelated with each other. The time instant at which the relative value of the (ϕ, θ) components of the first and second sources were equal to $(0, 1)$ and $(1, 1)$ was chosen, and the field map at this time instant was calculated. The noise was added to set the signal-to-noise ratio (SNR) of this simulated data equal to 25.

First, conventional minimum-norm reconstruction was performed using $\hat{f}(t_k) = L^{-1} b(t_k)$, where $L^{-1} = L^T (L L^T)^{-1}$. The field map obtained above was used and the reconstruction volume covers $-8 \leq x \leq 8$, $-8 \leq y \leq 8$, and $-2 \leq z \leq -8$. It consists of $17 \times 17 \times 7$ pixels. The plane, $y=1$, in the three-dimensional reconstruction is shown in Fig. 2. Here, the ϕ and θ components are separately displayed. These results clearly show that the minimum-norm method provides severely distorted three-dimensional reconstruction in this case. The covariance matrix of the measured data D was estimated from 500 data generations; This simulates data acquisition for 0.5 s with a sampling interval of 1 ms. The proposed Wiener reconstruction using Eq. (2) was applied with this covariance matrix. The results are shown in Fig. 3. Here, both sources are reconstructed, clearly demonstrating this method's three-dimensional reconstruction capability.

Next, sources having fixed orientations was reconstructed. In this experiment, the data used for obtaining D was generated assuming that the (ϕ, θ) components of the first and the second sources were fixed at $(0, 1)$ and $(1, 1)$, respectively. The results obtained using Eq. (2) are shown in Fig. 4. The ϕ component is correctly reconstructed. However, the reconstruction for the θ component contains severe distortion caused by non-diagonal terms that cannot be ignored. The results obtained using Eqs. (3) and (4) are shown in Fig. 5. Here, the two components are reconstructed. These results indicate that the effectiveness of Eqs. (3) and (4) for reconstructing sources with fixed orientations.

Conclusion

This paper proposes a method based on the principle of generalized Wiener estimation for obtaining a three-dimensional biocurrent distribution from spatio-temporal biomagnetic data. The method is formulated under the assumption that current sources are uncorrelated, and the method is extended to reconstruct current sources with fixed orientations. Computer simulation shows that the proposed method can reconstruct three-dimensional current distribution where the conventional least-squares minimum-norm method fails.

Acknowledgment

The authors wish to acknowledge Dr. A. Oppelt for the helpful discussion and for his encouragement to proceed this work.

References:

- [1] Hämäläinen, M.S. and Ilmoniemi, R.J., "Interpreting measured magnetic fields of the brain: Estimates of current distributions," Helsinki University of Technology, Report TKK-F-A559, 1984.
- [2] Jeffs, B., Leahy, R., and Singh, M., "An evaluation of methods for neuromagnetic image reconstruction", IEEE Trans. Biomed. Eng., 1987, 34: 713-723.
- [3] Kay, S.M., Fundamentals of Statistical Signal Processing: Estimation Theory, Englewood Clifles, New Jersey, Prentice-Hall, Inc., 1993.

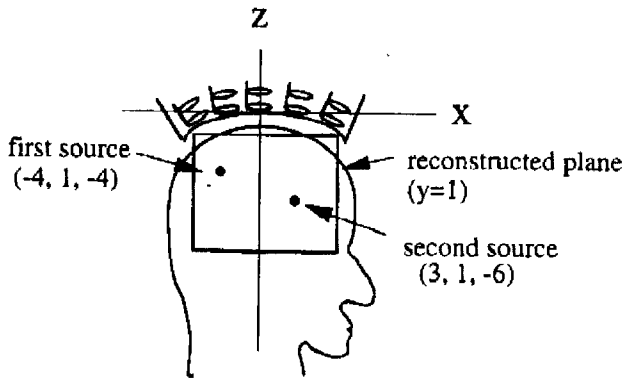


Fig. 1 Source current configuration assumed in computer simulation.

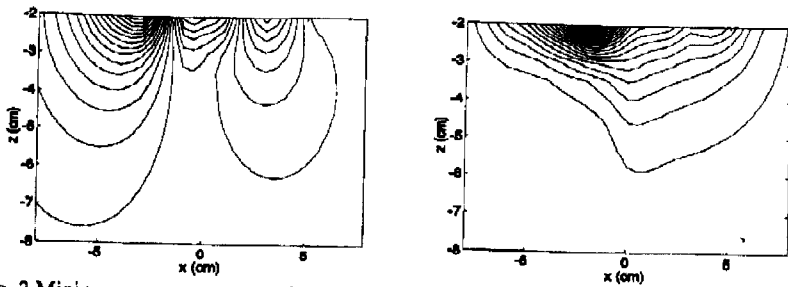


Fig. 2 Minimum norm reconstruction results.
Distribution of θ component (left) and that of ϕ components (right).

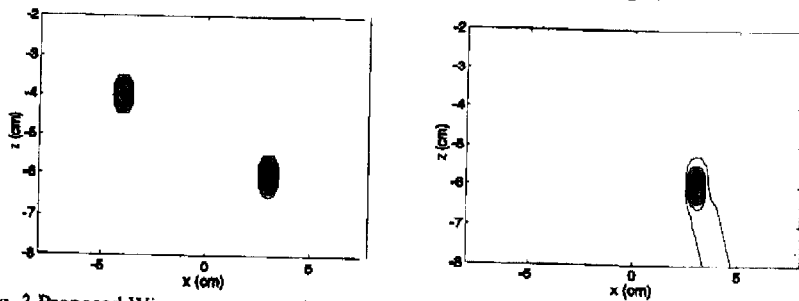


Fig. 3 Proposed Wiener reconstruction results.
Distribution of θ component (left) and that of ϕ components (right).

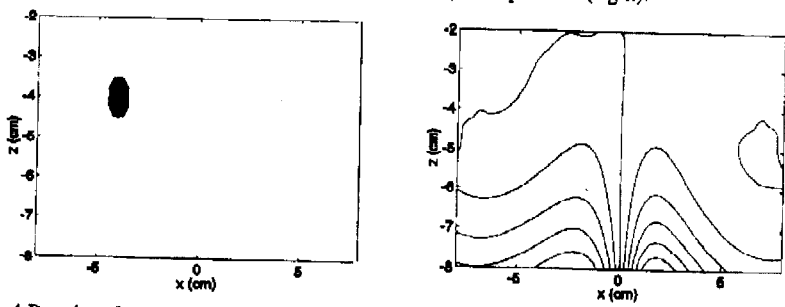


Fig. 4 Results of reconstruction with Eq. (2) for fixed orientation sources.
Distribution of θ component (left) and that of ϕ components (right).

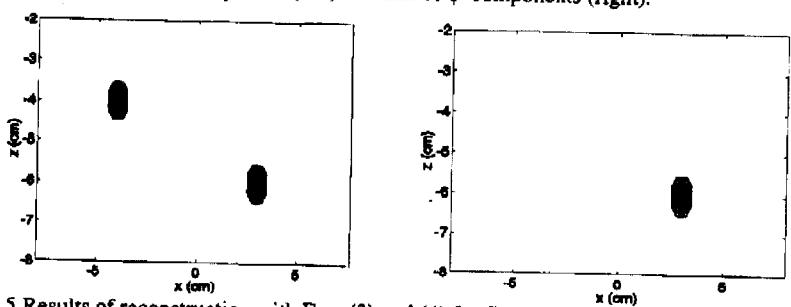


Fig. 5 Results of reconstruction with Eqs. (3) and (4) for fixed orientation sources.
Distribution of θ component (left) and that of ϕ components (right).